Stabilization of Tangent and Normal Contact Forces for a Quadrotor Subject to Disturbances

Carlos Izaguirre-Espinosa, A.J. Munoz-Vazquez, Anand Sanchez, Vicente Parra-Vega, R. Garcia Rodriguez, Pedro Castillo Garcia, D. Arreguin Jasso

Stabilization of Tangent and Normal Contact Forces for a Quadrotor subject to Disturbances

C. Izaguirre-Espinosa[1], A. Muñoz-Vazquez[2], A. Sánchez-Orta[3], V. Parra-Vega[3], R. Garcia-Rodriguez[4], P. Castillo[5], D. Arreguín-Jasso[3].

***Abstract*— Force exertion, object manipulation, and interaction are novel trending research topics of autonomous flying robots that can yield hoovering. Moreover, specifically with quadrotors, the vibration caused by the high natural frequency of rotating propellers exacerbates the problem of maintaining contact and exerting force against a rigidly fixed object. This contact vibration transfers back kinetic energy to the quadrotor that, in worst-case scenarios, surpasses its flying capabilities, which may lead to a crash. This paper studies the problem of aerial contact stabilization of a quadrotor equipped with a hemispherical deformable tip, which accommodates contact forces at a lower frequency. Thus two phenomena not studied in the literature arise: the rolling motion, and the deformation at contact. The contact force stabilization restores the effects of deformation while simultaneously endowing rolling by controlling a tangent constrained force. A model-free continuous attitude fractional controller to guarantee finite-time attitude stabilization is proposed. The residual coupled nonlinear dynamics yields the desired attitude corresponding to a given contact force; thus, force stabilization is achieved. Finally, experimental results are presented to assess the performance of the proposed approach.**

I. Introduction

Recently, there has been great interest in the development of theoretical and experiments of quadrotor's goal to interact with the environment, or to manipulate cooperatively an object. These tasks involve force control approaches [1]–[3]. However, these approaches are based on ideal assumptions, such as either infinitesimal contact point models that likely lead to high-frequency interactions, which jeopardize the fragile quadrotor structure, or assuming system's exact knowledge, thus the model becomes sensitive to parametric uncertainty. To circumvent the limitation of using infinitesimal point contact mechanics, there has been considered a contact area that leads to a moving pressure point nonetheless, or deformable contact pad, violating their design assumptions. Others study contact throughout attaching of a rigid manipulator to the quadrotor. If the contact occurs below or above the CoM, a careful operation is required due to zero dynamics being unstable [4]. When placing the manipulator above, the hybrid force scheme decouples Cartesian coordinates of force and velocity, then embeds dynamics in independent velocity coordinates, [5], [6]. Interestingly, [7] considers an impedance force model in the normal direction, with tangent friction component, when contacting with a perch on top of the quadrotor frame. Contact force is stabilized separately using a disturbance observer; however, it lacks of a complete stability analysis, [8]. Despite the practical advantages of introducing a deformable passive damper as the tip to avoid troublesome vibrations at contact, engaging contact with such deformable soft tip against a rigid surface has not been studied formally for underactuated constrained quadrotors. Therefore, we abstract this as the problem of force stabilization subject to a hemispherical deformable tip that yields a moving contact point while rolling, a problem that remains elusive in the literature.

1) Our Proposal: When contact occurs with a given force exertion between a curved soft tip and a rigid object, a contact area arises; then, there exists a pressure contact point where the maximum deformation arises. This point may move due to the curved tip that endows a rolling velocity, but simultaneously there arises a normal force due to deformation. This phenomena introduces a constraint tangent force that enforces a velocity constraint, which is nonholonomic for the general case. Although the inclusion of the normal and tangential forces has several advantages for critical quadrotor contact tasks, its study has been neglected in the literature.

In contrast to previous works, our paper explicitly considers such constraints without any linearization, [9], it proposes a model-free continuous attitude controller that stabilizes quadrotor contact when interacting with curved soft tip against a rigid object. Motivated by robotic hands equipped with soft fingertips, [10], the contact force is applied throughout a deformable hemispherical tip. Then, a fast and robust controller is proposed to enforce a quasi-hovering state which endows an analysis restricted to the xz plane. It is shown that contact force

[1] Faculty of Chemistry Sciences, Autonomous University of Nuevo Leon, Mexico. Email: carlos.izaguirresp@uanl.edu.mx

[2] College of Engineering, Texas A&M Univ., McAllen, USA. Email: aldo@gmail.com

[3] Robotics and Advanced Manufacturing Division, Center for Research and Advanced Studies (Cinvestav), Saltillo, Mexico. Email: (anand.sanchez, vparra, daniel.arreguin)@cinvestav.mx

[4] Aeronautical Engineering Program and Postgraduate Program in Aerospacial Engineering, Universidad Politecnica Metropolitana de Hidalgo, Mexico. Email: rogarcia@upmh.edu.mx

[5] Sorbonne Universités, Université deTechnologie de Compiégne, CNRS UMR 7253 Heudiasyc Lab., CS 60319, 60203 Compiégne Cedex, France. Email: pedro.castillo@hds.utc.fr

depends on pitch angle, thus such angle is controlled in finite-time to finally guarantee exerting the desired force. In this way, our scheme stands for an active force control for constrained quadrotors subject to a rolling constraint, assuming that contact occurs with a deformable curve surface to stabilize normal and tangential forces.

II. Quadrotor Dynamic Model Subject to a Velocity Constraint

A. Motivation to Introduce a Deformable Contact Tip

A quadrotor that performs contact tasks with a deformable contact tip is characterized by kinetic energy absorbed by elastic deformation. So the kinetic energy at impact is of lesser magnitude, acting also as a low pass filter that damps enormously and rapidly (faster than the closed-loop response of the control system) the contact forces, producing a natural frequency within the limits of design. Although the Hunt-Crossley contact force model is consistent with the intuitive notion of a constitutive force that depends on the restitution coefficient plus viscous damping, which represents the net energy loss during impact, [11]. An adaptation of Hooke's law for hemispherical shape contact has been extensively validated for deformable fingertip, [12], however at the expense of introducing a Pfaffian velocity constraint due to tip rolling, which has been overlooked in the literature on quadrotors in contact tasks.

To model such phenomena, let the quadrotor be equipped with a hemispherical soft tip to engage contact with a rigid surface. Thus the hemispherical shape of radius R yields a varying contact point when rolling onto the rigid surface, see Fig. 1(a). Hence, the rolling constraint velocity can be modeled by $\dot{\varphi} = \dot{z}_c - R\dot{\theta} = 0$, where z_c is the contact altitude in $z = z_c - l\sin(\theta)$, for pitch angle θ and the length l defined as the distance from CoM to the contact point, then $\dot{z} = \dot{z}_c - l\cos(\theta)\dot{\theta}$. Thus, the rolling constraint velocity is given as follows

$$\dot{\varphi} = \dot{z} + (l\cos(\theta) - R)\dot{\theta} = J_\varphi \dot{\gamma} \equiv 0 \tag{1}$$

where $J_\varphi = [0 \quad 0 \quad 1 \quad 0 \quad (l\cos(\theta) - R) \quad 0]$, and $\dot{\gamma} = \left[\dot{x}, \dot{y}, \dot{z}, \dot{\phi}, \dot{\theta}, \dot{\psi}\right]^T$ is the time derivative of $\gamma = [\xi^T, \eta^T]^T \in \mathbb{R}^6$, for position $\xi = [x, y, z]^T \in \mathbb{R}^3$, and Euler angles $\eta = [\phi, \theta, \psi]^T \in \mathbb{R}^3$. The linear operator J_φ stands for the annihilator of velocities $\dot{\gamma}$ at contact, thus qualifying as the Pfaffian matrix of the constraint at contact (1). Notice that, in general, $J_\varphi \in \mathbb{R}^{r\times 6}$, for r the number of independent contacts (in our case, $r = 1$), spans the tangent subspace at contact. For convenience, J_φ can be written $J_\varphi = [J_{\varphi z}, J_{\varphi\theta}]^T$, where $J_{\varphi z} = [0, 0, 1]^T$ and $J_{\varphi\theta} = [0, (l\cos(\theta) - R), 0]$ represent the gradient of the rolling constraint with respect to z and θ, respectively. Thus, using the principle of virtual work and variational calculus, a workless constrained force $\lambda \in \mathbb{R}^r$ (a Lagrangian multiplier) appears that enforces the constraint (1). That is, λ is a non-dissipative tangent force along the span of J_φ^T that enforces the constraint and prevents slipping within the limits of the Coulomb friction coefficients. Based on the arguments above, it is compulsory to control λ to enforce the velocity constraint from the tip rolling at contact.

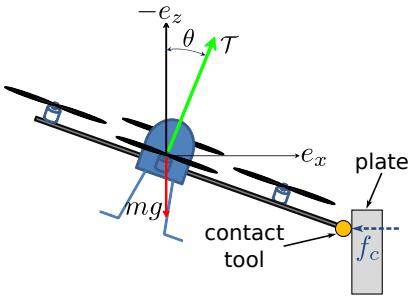

(a) Lateral view of the quadrotor in constrained pose.

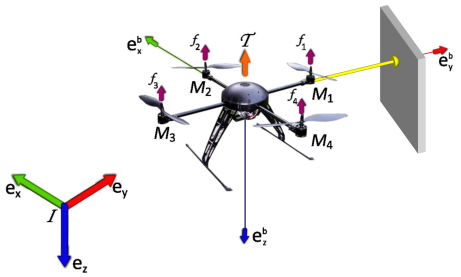

(b) The constrained quadrotor system and frames.

Fig. 1. The quadrotor performing a contact task with a deformable contact tip.

B. Dynamic Model subject to Pfaffian Constraints and to Disturbances

Let $\mathcal{I} = \{\hat{e}_x, \hat{e}_y, \hat{e}_z\}$ and $\mathcal{A} = \{\hat{e}_x^b, \hat{e}_y^b, \hat{e}_z^b\}$ denoting the inertial (Earth) and body fixed frame of quadrotor, respectively, Fig. 1(b). The quadrotor is represented as an airborne rigid body subject to a force and 3 moments

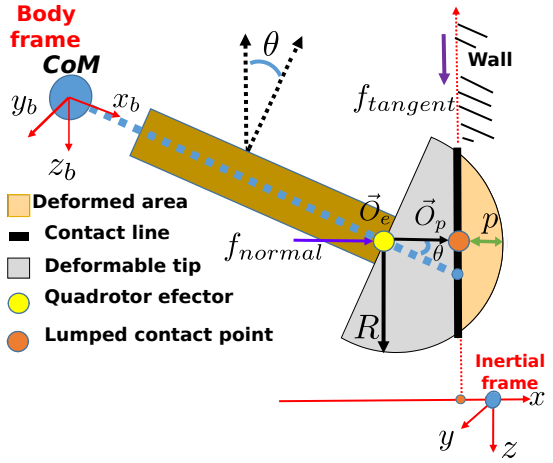

Fig. 2. Details of the quadrotor at contact with a soft hemispherical tip: normal and tangential forces arise due to elastic deformation of tip material at contact.

produced from the thrust of the four rotors located at equidistant length c, with respect to the center of mass (CoM) that coincides with the origin of $\mathcal{A}$, which is also the geometric center, see Fig. 1(b), [13]. Since the quadrotor has a hemispherical soft tip as the contact tool, collinear to x-axis, the quadrotor is constrained to the xz-plane, then deformation of soft tip arises along the x-axis, see Fig. 1(a). Thus, there exists a maximum penetration depth p due to the deformation, measured along the line $\vec{O}_p - \vec{O}_e$, given by $p = R - D_x$, where D_x stands for the distance of the center position of the contact tool to the lumped contact point, see Fig. 2. In addition, Fig. 2 shows that the CoM coincides with the origin of the coordinate system associated to the body fixed frame. However, notice that the contact point $\vec{O}_p$ is unknown. Therefore, the contribution of the pitching constraint is measured from $\vec{O}_e$, taking the effect at θ. Thus, the Newton-Euler constrained dynamic equations are given by

$$m\ddot{\xi} = -\mathcal{T}\mathcal{R}\hat{\mathbf{e}}_z^b - F_c + J_{\varphi z}^T\lambda + mg\hat{\mathbf{e}}_z + d_\xi \quad (2)$$

$$\dot{\mathcal{R}} = \mathcal{R}[\Omega\times] \quad (3)$$

$$J\dot{\Omega} = -\Omega \times J\Omega + \tau + L \times \mathcal{R}^T F_c + W^{-T} J_{\varphi\theta}^T \lambda + d_\eta \quad (4)$$

subject to $\dot{\varphi} = 0$, where $J \in \mathbb{R}^{3\times3}$ denotes the constant inertia matrix with respect to the CoM expressed in the body fixed frame $\mathcal{A}$, $\xi \in \mathcal{I}$ denotes the operational position coordinates of the CoM of the airframe, relative to a fixed origin, $F_c = f_c\hat{\mathbf{e}}_x$ stands for the contact force with magnitude f_c, $\mathcal{R} \in SO(3)$ is a rotation operator, $\Omega = [\Omega_x, \Omega_y, \Omega_z]^T \in \mathcal{A}$ represents the angular velocity of the airframe, which is related to Euler angles velocities, $\dot{\eta}$, through the transformation matrix W as $\Omega = W\dot{\eta}$. $\mathcal{T} = f_1+f_2+f_3+f_4 \in \mathbb{R}_+$ stands for the thrust generated by rotors' forces, where $f_i = \kappa_p\omega_i^2$, $\kappa_p > 0$, and ω_i is the angular velocity of each motor. Let $L = l\hat{\mathbf{e}}_x^b$ the vector from the CoM to the contact point, g the gravitational acceleration, and m denotes the mass of the quadrotor. The term $[\Omega\times]$ denotes the skew-symmetric matrix of Ω, d_ξ, d_η represent smooth bounded disturbances, and $\tau = [\tau_\phi, \tau_\theta, \tau_\psi]^T \in \mathbb{R}^3$ in $\mathcal{A}$, is the control torque. Therefore, at this point, the control problem is to *design the 4-dimensional* $[\mathcal{T}, \tau^T]^T$ *to stabilize the underactuated 6-dimensional disturbed quadrotor* (2)-(4) *in contact at* $\vec{O}_e$ *and subject to* (1)*, while exerting a given desired constant force* f_{c_d}.

C. Contact Force Model

Consider a lossless elastic deformable tip of the quadrotor, see Fig. 2, then the hemisphere shape of homogeneous material of constant density yields a restitution force f_c along x given by, [10],

$$f_c = f_c(p) = \frac{E_Y p^2}{\cos(\theta)} \quad (5)$$

where E_Y stands for the elastic Young modulus coefficient of the soft tip material, then constant in the linear zone, which can be characterized in prior experiments. It is now clear to discern that commanding θ in (5) will command the value of f_c, which we pursue next.

III. Control Design

A. Fractional Sliding Mode Attitude Control

Assuming the exerted force f_c is orthogonal to the z-axis, then without loss of generality assume that there arises along the x-axis an explicit dependence of f_c with pitching angle θ, in accordance to (5); then, the desired Euler angles may be chosen $\eta_d = (0,\ \theta_d,\ 0)^T$, for a desired pitch angle θ_d. Given the parametric and model uncertainties of position (2) and attitude dynamics (4), and inspired by [14], let the following model-free fractional sliding mode controller [15] for attitude control be

$$\tau = -k\ {}_{t_n}I_t^\nu \text{sign}(S_\Omega), \quad (6)$$

where $k > 0$ is a feedback gain, $\text{sign}(\cdot)$ the discontinuos signum function, S_Ω the attitude error manifold given by

$$S_\Omega = \Omega_e + \alpha\mathcal{R}_d^T q_e, \quad (7)$$

for $\alpha > 0$ a positive constant, $\Omega_e = \Omega - \Omega_d$ represents the angular velocity error, where $\Omega_d = W(\eta_d)\dot{\eta}_d$ is the desired angular velocity, corresponding to a desired rotation matrix $\mathcal{R}_d$ and a desired quaternion $\mathbf{q}_d$, and $\mathbf{q}_e = (q_{0e}, q_e) = \mathbf{q} \otimes \mathbf{q}_d^* = (q_0, q) \otimes (q_{0d}, -q_d)$ with $q_0, q_{0d}, q_{0e} \in \mathbb{R}$ and $q, q_d, q_e \in \mathbb{R}^3$. The term ${}_{t_n}I_t^\nu$ is the Riemann-Liouville fractional differintegral operator given by, [16], ${}_aI_t^\nu f(t) = \frac{1}{\Gamma(\nu)}\int_a^t (t-\varsigma)^{\nu-1} f(\varsigma)d\varsigma$ for $\nu \in [0, 1)$ the fractional order of the fractional integral, $f(t)$ is a locally integrable function, $\Gamma(\nu)$ stands for the Gamma function, i.e. $\Gamma(\nu+1) = \nu!$ for $\nu \in \mathbb{N}_0$.

Now, consider the open-loop attitude error

$$J\dot{S}_\Omega = \tau + d_\Omega \quad (8)$$

with $d_\Omega = -J(\Omega_d - \alpha\mathcal{R}_d^T q_e) - \Omega \times J\Omega + L \times \mathcal{R}^T F_c + W^{-T}J_{\varphi\theta}^T\lambda + d_\eta$ the lumped function of all model and parametric uncertanties, as well as disturbances. The stability properties of (8) in closed-loop with attitude controller (6) are given in the following Theorem.

Theorem 1: Model-free Fractional Attitude Control. *Consider* (8) *in closed-loop with* (6)*. For* $k > J_{ii}^{-1}\frac{3+\nu}{1-\nu}\max_i \sup_{(a,b)} \frac{|d_{\Omega i}(b) - d_{\Omega i}(a)|}{(b-a)^\nu}$, $\exists t_f < \infty$ *such that* $S_\Omega(t) = 0$, $\forall t \geq t_f$*, where* J_{ii} *stands for the ii element of* J*.*

Sketch of the Proof. Following our previous basic results on fractional sliding modes, [14], [15], [17], [18] one can easily follow developments to conclude the invariant manifold $S_\Omega = 0$ is reached in finite time t_f, then afterwards tracking error $\mathbf{q}_e \to (1, [0,0,0]^T)$ converges exponentially, so does $\eta \to \eta_d$. In consequence, after $t > t_f$, coordinates $\phi = \psi = 0$ and $\theta = \theta_d$ exponentially fast in accordance to k and ν. Be aware that the fractional-order integral acts as a low-pass filter, whose gain and phase are modulated via $\nu \in [0, 1)$, still preserving stability and robustness properties against attitude lumped

disturbances d_Ω of (8), even if it were non-differentiable, the interested reader is referred to [14], [15], [18] for an in-depth proof of the later claim. □

B. Force Control Design

1) Design of Desired Pitch Angle: Let us consider that at initial condition, there exists stable contact and then a hovering state induced by the attitude control τ, where $\phi = \psi = 0$ and $\theta = \theta_d \approx 0$. The force control task is to exert f_{c_d} along x onto the rigid surface, see Fig.1(a), then we have that $x = x_c - l\cos(\theta)$, $z = z_c - l\sin(\theta)$, where x_c and z_c represent the center position of the contact tool in the x and z axes, respectively. In this condition, position dynamics given by (2) becomes

$$m\ddot{x} = -\mathcal{T}\sin(\theta) + f_c + d_x \quad (9)$$

$$m\ddot{z} = -\mathcal{T}\cos(\theta) + mg + \lambda + d_z \quad (10)$$

where f_c represents the normal force acting along x, see Fig. 2, d_x and d_z are respectively the x and z components of disturbance d_ξ, and λ is the tangent force along z. Solving for $\mathcal{T}$, (9)-(10) leads to, [19], $\tan(\theta) = \frac{f_c - m\ddot{x} + d_x}{m(g-\ddot{z})+\lambda+d_z}$. Then, we have

$$\theta = \frac{f_c}{mg} + d_\theta \quad (11)$$

for $d_\theta = \frac{mg(d_x - m\ddot{x}) + (m\ddot{z} - d_z)f_c}{mg[m(g-\ddot{z})+\lambda+d_z]} + [\theta - \tan(\theta)]$. Observe how θ is function of f_c in (11), whose explicit relation can be exploited to design θ_d to be a function also of the desired contact force f_{c_d} along x. Take note that in quasi-hovering state[1] $\phi = \psi = 0$ and $\theta = \theta_d \approx 0$, then also $\ddot{x} \approx \ddot{z} \approx 0$ and that $\tan(\theta) \approx \theta$ needs to be enforced to ameliorate the effects of d_θ. Moreover, from (5) and (11) and considering that $\cos(\theta) \approx 1$ for such small angles, we have that

$$\theta = \frac{f_c}{mg} \quad (12)$$

where $f_c = E_Y p^2$. Henceforth, in this condition, the desired pitch angle becomes

$$\theta_d = \frac{f_{c_d}}{mg}. \quad (13)$$

2) Design of the Force Controller (a.k.a. the Controller of Pitch): From (12)-(13), one obtains

$$\Delta\theta = \frac{\Delta f_c}{mg} + d_\theta \quad (14)$$

for $\Delta\theta = \theta - \theta_d$ and $\Delta f_c = f_c - f_{c_d}$. Since the attitude controller enforces fast convergence of $\eta \approx 0$, one has that $q \approx \frac{1}{2}\eta$, and $R \approx W \approx I$, where I is the 3×3 identity matrix; then, (7) can be approximated by

$$S_\theta = \Delta\dot{\theta} + \frac{1}{2}\alpha\Delta\theta, \quad (15)$$

Replacing each term in the right hand side of (15) by (14) and its derivative, (15) can also be approximated in quasi-hovering by $S_f = \frac{\Delta\dot{f}_c}{mg} + \frac{1}{2mg}\alpha\Delta f_c$. Taking the time derivative of (15) and from (4), one obtains

$$\dot{S}_f = \tau_\theta + d_f \quad (16)$$

where d_f accounts for disturbances to the force dynamics. On that account and consistently with Theorem 1, the controller τ_θ becomes

$$\tau_\theta = -k\ {}_{t_{nf}}I_t^\nu \mathrm{sign}(S_f), \quad (17)$$

Then, we have proved the following assertion.

Corollary 1: Consider the controller (17) in closed loop with (16), then one obtains $\dot{S}_f = -k\ {}_{t_{nf}}I_t^\nu \mathrm{sign}(S_f) + d_f$, which according to Theorem 1, there arises the finite-time convergence of S_f, with exponential stabilization of contact force bounded by a vicinity given by $\|\Delta f_c\|_{\mathcal{L}^2} \leq \frac{2mg}{\alpha}\left\|f\left(d_\theta, \dot{d}_\theta\right)\right\|_{\mathcal{L}^2}$, where $f\left(d_\theta, \dot{d}_\theta\right)$ is a function that accounts for disturbances induced by d_ξ and the dynamics of the contact forces.

Remark 1: The precision of force tracking can be modulated by tuning the feedback gain α. Additionally, the use of $\dot{\theta}(t)$ instead of $\dot{f}_c(t)$ sacrifices the exponential convergence of Δf_c at the expense of obtaining finite-gain input-output stability, [20], which from a practical point of view, it is convenient since signal $\theta(t)$ is more regular than signal $f_c(t)$, on one hand, but then the force sensor is not needed, on the other hand.

IV. Experimental Study

1) Setup: An Optitrack motion capture system provided measurements of the state of the quadrotor, a Parrot AR Drone 2.0 of 0.458Kg weight, handled by a Desktop PC throughout wireless communication by Gumstix processing ports, while a second PC handled the data from the JR3 multi-axis force sensor, then transmitted this data to the Desktop PC. The specific details about the firmware structure of this platform, the finesse in its tuning, including sensors and rate of data transfer, can be found in [18]. The contact point is computed using the length of the contact tool at initialization, from therein the positive x direction. The contact tool, seen in Fig. 3, was made of carbon fiber and is rigidly attached to the frame of the Parrot AR Drone, equipped with a rigid rod covered with a deformable sponge to provide a circular shape at contact.

2) Tuning Gains: The Grünwald-Letnikov method computed the numerical differintegrals with a buffer of 5000 elements. The differintegration order, ν, plays a critical compromise in disturbance rejection with how aggressive the control signal is. Previous to the force experiments[2], the tuning of control gains for the position and attitude controller were obtained. It was calculated that $\nu = 0.5$ since $\nu < 0.5$ generates an aggressive signal that endangered rotors' integrity, while $\nu > 0.5$ creates a phase delay high enough for the force disturbances to

[1]This is physically reasonable to consider in force control of quadrotors because such configuration is the only one the quadrotor can compensate its own weight.

[2]Experiments have been conducted in the Heudiasyc Laboratory at the Université de Technologie de Compiègne, France.

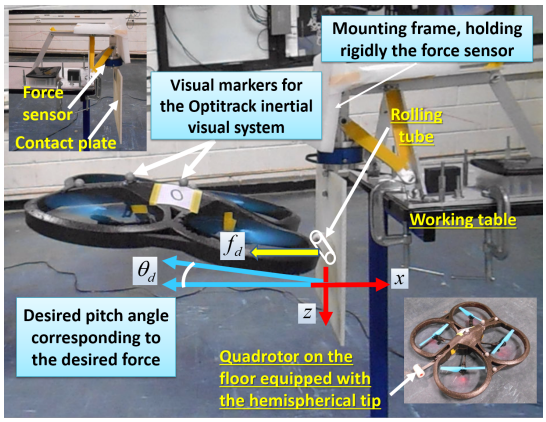

Fig. 3. Experimental testbed showing quadrotor in contact to a nylamid contact plate. The $JR3-90M31$ force sensor, rigidly attached to an aluminum-made working table, measures online 6D wrench at $1KHz$, while visual markers provided the distinctive visual features to measure the quadrotor state. Final sampling rate was $h = 10ms$.

destabilize the quadrotor beyond recovery. Notice that since we assumed no knowledge of the tip deformation, a parametric uncertainty in the compliance behavior produced a small uncertainty at the initial position, an issue dealt with by the robust force controller. Remaining control gains were $\alpha = 9$, and $k = 0.6$. For the flight tests is proposed that $f_d = 0.79N$ and $\theta_d = -10^o$, at the contact point $[x_c, y_c, z_c] = [0, 0, -0.75]m$, which is the center of the contact plate, see Fig 4, thus $[x_d, y_d, z_d] = [0.01, 0, -0.8]m$.

3) Results: Fig. 4(c) shows how difficult it was to regulate ψ, due to the resulting torque yielded contact vibration as expected with a f_c, exciting also a residual moment in yawing. Continuous control signals provide robustness against disturbances, as shown in Fig. 5.

Successful regulation of force is accomplished, as depicted in Fig. 6, wherein the $\pm 1\%$ of force sensor noise is observed where quadrotor vibrations are damped out by the soft material of the tip of the rod. Fig. 6 also shows how the quadrotor rejects disturbances since the beginning of the operation.

V. Conclusions

Two phenomena largely used in practice [21], but also neglected in the literature as adding a hemispherical deformable tip to the quadrotor to establish contact with rigid smooth surface, have been studied in this paper. Consequently, we explicitly addressed the tip rolling and tip deformation. Such setup damps contact at the expense of introducing a rolling velocity constraint at contact, also neglected in the literature of quadrotor. The novel model-free yet robust fractional proposed controller stabilizes the full nonlinear aerodynamics, including disturbances. Experiments show that the capacity to exert forces is compromised by mass, thrust, and the desired force (in the underactuated directions), altogether by the radius and Young modulus of the deformable tip. Overall, assuming full access to the state as customary, our controller is easy to implement by virtue of its model-free structure that requires only the integral of signum of attitude error manifold. Moreover, force sensing is not strictly required since the force model, prior characterization, can compute it. Finally, it is worth mentioning that in [9], a variable substitution method for feedback linearization is used in order to assure 1D contact force by also using the dependence of pitch angle to desired force, somewhat similar in spirit to our proposal, but a different approach (our result is achieved without any linearization).

Acknowledgements

Authors acknowledge partial support from the programm Investissements d'avenir programme through the Robotex Equipment of Excellence Grant ANR-10-EQPX-44 of France, and the Labex MS2T Framework of France through the

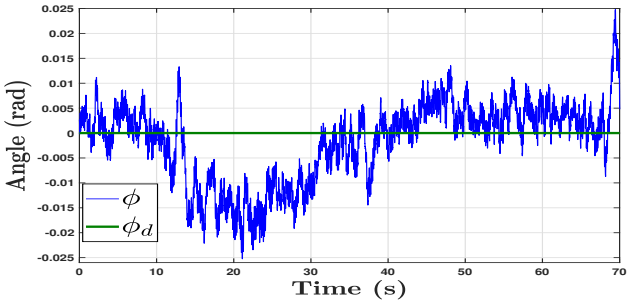

(a) Regulation at 0 of ϕ suffering from force disturbances.

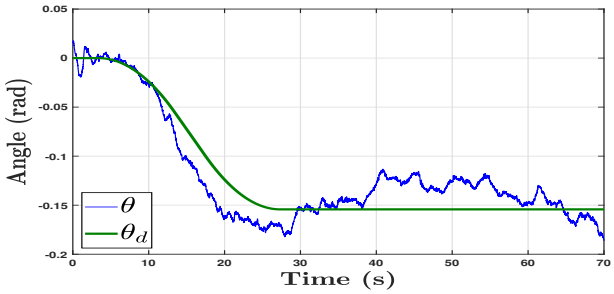

(b) Tracking of smooth θ_d leads to force regulation.

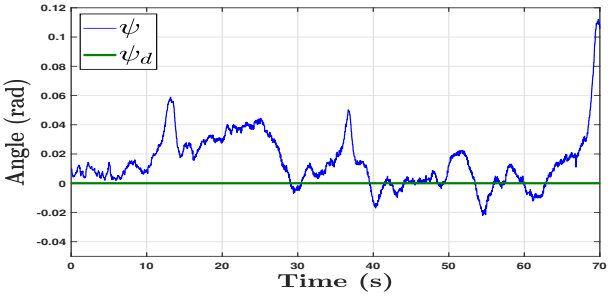

(c) Regulation in ψ suffers the most due to force and torques disturbances.

Fig. 4. Attitude of the quadrotor during force regulation.

program “Investments for the future” Grant ANR-11-IDEX-0004-02 of the National Agency for Research.

References

[1] D. Mellinger, M. Shomin, N. Michael, V. Kumar, Cooperative Grasping and Transport Using Multiple Quadrotors, Distributed Autonomous Robotic Systems, 83, pp. 545–558, 2013.

[2] M. Fumagalli, R. Naldi, A. Macchelli, R. Carloni, S. Stramigioli, and L. Marconi, Modeling and control of a flying robot for contact inspection, IEEE/RSJ Int. Conf. on Intell. Robots and Systems, 2012, pp. pp. 3532-3537.

[3] G. Gioioso, M. Ryll, D. Prattichizzo, H.-H. Bulthoff, and A. Franchi, Turning a Near-hovering Controlled Quadrotor into a 3D Force Effector, IEEE Int. Conf. on Robotics and Automation, pp. 6678-6284, 2014.

[4] H.-N. Nguyen, Ch. Ha, and D. Lee, Mechanics, control and internal dynamics of quadrotor tool operation, Automatica, 61, pp. 289–301, 2015.

[5] Y. Hayashi, D. Yashiro, K. Yubai and S. Komada, Experimental Validation of Contact Force Control of Quadrotor Based on Rotor Angular Acceleration Control, 2019 IEEE Int. Conf. on Mechatronics, pp. 684-689, 2019.

[6] T. Wang, K. Umemoto, T. Endo, and F. Matsuno, Dynamic hybrid position/force control for the quadrotor with a multi-degree-of-freedom manipulator, Artificial Life and Robotics, 24, pp. 378–389, 2019.

[7] X. Ye, Y. Liu, Ch. Huang, Modeling and Control based on a Force Observer for a Flying-perching Quadrotor, IEEE Annual Int. Conf. on CYBER Tech. in Aut.omation, Control, and Intell. Syst., pp. 758-763, 2018.

[8] W.-H. Chen, D.-J. Ballance, P.-J. Gawthrop, and J. O'Reilly, A nonlinear disturbance observer for robotic manipulators, IEEE Trans. on Industrial Electronics, 47(4):932-938, 2000.

[9] X. Meng, Y. He, Q. Wang, T. Yan and J. Han, Force-Sensorless Contact Force Control of an Aerial Manipulator System, IEEE Int. Conf. on Real-time Comp. and Robotics, pp. 595-600, 2018.

[10] R. Ozawa, S. Arimoto, P.-T.-A. Nguyen, M. Yoshida, and J.-H. Bae, Manipulation of a Circular Object in a Horizontal Plane by Two Finger Robot, IEEE Int. Conf. on Robotics and Biomimetics, pp 517–522, 2004.

[11] K. Hunt and F. Crossley, Coefficient of restitution interpreted as damping in vibroimpact, ASME J. Appl. Mech., 1975, 42, pp. 440-445, 1975.

[12] Y. Matsuzaki, K. Inoue, and S. Lee, Manipulation of micro-scale objects using micro hand with two rotational fingers, Int. Symp. on Micro-NanoMechatronics and Human Science, pp. 438-443, 2009.

[13] B. Etkin, and L. Reid, Dynamics of Flight: Stability and Control, New York, Wiley, 1996.

[14] A.-J. Muñoz-Vázquez, V. Parra-Vega and A. Sánchez-Orta, Continuous fractional sliding mode-like control for exact rejection of non-differentiable Hölder disturbances, IMA Journal of Mathematical Control and Information, p. dnv064, 2015.

[15] C. Izaguirre-Espinosa, A. J. Muñoz-Vázquez, A. Sánchez-Orta, V. Parra-Vega, and P. Castillo, Attitude Control of Quadrotors based on Fractional Sliding Modes: Theory and Experiments, IET Control Theory & Applications, 10(7), pp. 825–832, 2016.

[16] Podlubny, I. *Fractional Differential Equations*, San Diego CA: Academic Press, 1999.

[17] A. Sanchez-Orta, V. Parra-Vega, C. Izaguirre-Espinosa, and O. Garcia, Position-Yaw Tracking of Quadrotors, J. of Dynamic Systems, Measurement, and Control, 137(6): 061011, 2015.

[18] C. Izaguirre-Espinosa, A.-J. Muñoz-Vázquez, A. Sánchez-Orta, V. Parra-Vega, P. Castillo, Contact force tracking of quadrotors based on robust attitude control, Control Engineering Practice, vol. 78, pp. 89-96, 2018.

[19] C. Izaguirre-Espinosa, A. J. Muñoz-Vázquez, A. Sánchez-Orta, V. Parra-Vega and G. Sanahuja, Fractional Attitude-reactive Control for Robust Quadrotor Position Stabilization without Resolving –Underactuation, Control Engineering Practice, 53, pp. 47-56, 2016.

[20] G. Zames, On the input-output stability of nonlinear time-varying feedback systems, Part I. IEEE Trans. on Automatic Control, 11, pp. 228-238, 1996.

[21] G. Darivianakis, K. Alexis, M. Burri and R. Siegwart, Hybrid predictive control for aerial robotic physical interaction towards inspection operations, IEEE Int. Conf. on Robotics and Automation, pp. 53-58, 2014.

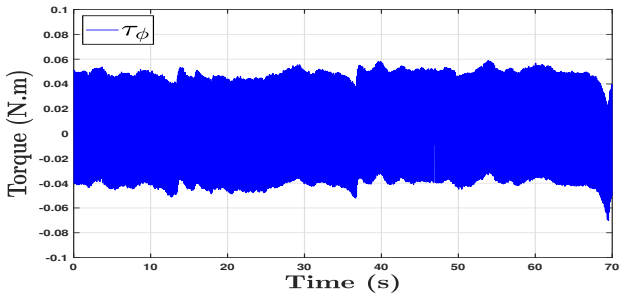

(a) Regulation at 0 of ϕ suffering from force disturbances.

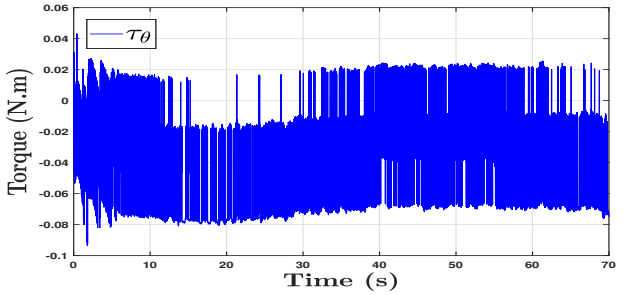

(b) Tracking of smooth θ_d leads to force regulation.

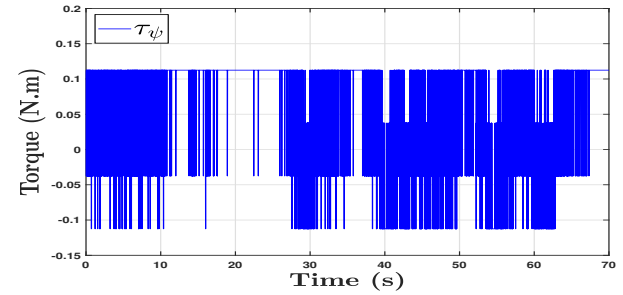

(c) Regulation in ψ suffers the most due to force and torques disturbances.

Fig. 5. Control signals during experiments.

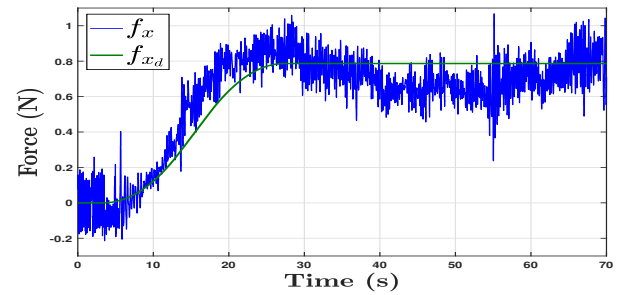

Fig. 6. Force regulation at $f_d = 0.72N$.